Transient Variability In Vapor Intrusion And The Factors That Influence It

Jonathan G. V. Ström,[†] Yijun Yao,[‡] and Eric M. Suuberg[*,†]

†*Brown University, School of Engineering, Providence, RI, USA*

‡*Zhejiang University, Hangzhou, China*

E-mail: eric_suuberg@brown.edu

Abstract

Temporal variability in indoor air contaminant concentrations at vapor intrusion (VI) sites has been a concern for some time. We consider the source of the variability at VI sites located near Hill Air Force Base and Naval Air Station North Island using statistical analysis methods and three-dimensional subsurface computational fluid dynamics modeling. The results suggest that an order of magnitude variation in indoor air contaminant concentrations may be expected at "normal" VI sites where preferential pathways do not play a role, whereas three or more orders of magnitude can be observed at sites characterized by preferential pathways. A CFD modeling sensitivity analysis reveals that it is not only the presence of contaminant vapor in a preferential pathway that is required to see large observed variations, but there must also exist a permeable region beneath the structure. Large temporal fluctuations in indoor air contaminant concentrations may be observed where no preferential pathways exist, but this requires a particular combination of large fluctuations in pressure driving force and high soil permeability.

Introduction

Long term vapor intrusion (VI) studies in both residential and larger commercial structures have raised concerns regarding significant observed transient behavior in indoor air contaminant concentrations.[1–6] VI involves the migration of volatilizing contaminants from soil, groundwater or other subsurface sources into overlying structures. VI has been a recognized problem for some time, but many aspects remain poorly understood, particularly with respect to the causes of large temporal transients in indoor air concentrations. There is uncertainty within the VI community regarding how to best develop sampling strategies to address this problem.[1,3,7]

Results from a house operated by Arizona State University (ASU) near Hill AFB in Utah, an EPA experimental house in Indianapolis, IN and a large warehouse at the Naval Air Station (NAS) North Island, CA have all shown significant transient variations in indoor air contaminant concentrations. All were outfitted with sampling and monitoring equipment that allowed tracking temporal variation in indoor air contaminant concentrations on time scales of hours. All have shown that these concentrations varied significantly with time - orders of magnitude on the timescale of a day or days.[5,8,9]

In one instance the source of the variation was clearly established during the study; at the ASU house a field drain pipe (or “land drain”), which connected to a sewer system, was discovered beneath the house, and careful isolation of this source led to a clear conclusion that this preferential pathway significantly contributed to observed indoor air contaminant levels and their fluctuations.[9,10] While in this case the issue of a contribution from a preferential pathway was clearly resolved, what it left open was a question of whether existence of such a preferential pathway to an area beneath a structure would always be expected to lead to large fluctuations in indoor air contaminant concentrations.

Similarly, a sewer pipe has recently been suggested to be a source of the contaminants found in the EPA Indianapolis house.[11] That site was also characterized by large indoor air contaminant concentration fluctuations. Sewer lines have been generally implicated as VI source at several sites to date.[11–14] A Danish study estimates that roughly 20% of all VI sites in central Denmark involve significant sewer VI pathways.[15] Thus while the consideration of a role of possible sewer or other preferential pathways is now part of normal good practice in VI site investigation, it is still not known whether the existence of such pathways automatically means that large temporal fluctuations are necessarily to be expected. In some of these cases,[12,14] the sewer provided a pathway for direct entry of contaminant into the living space. While potentially important in many cases, this scenario is not further considered here, where the focus is on pathways that deliver contaminant to the soil beneath a structure.

It is, however, now known that even absent a preferential pathway, there may be significant transient variation in indoor air contaminant concentrations at VI sites.[2,4,16] One example is a site at NAS North Island at which no preferential pathways have been identified. Instead, a building at this site is characterized by significant variations in indoor-outdoor pressure differential.[5] It is believed that this is the origin of the fluctuations at that site.

This paper investigates the sources of the temporal variation in indoor air contaminant concentrations in both the presence and absence of in soil preferential pathways. In this work, the latter scenarios are referred to as "normal" VI scenarios, in which there is typically a groundwater source of the contaminant. Specifically, we pose the question of just how much variation in indoor air contaminant concentration may be expected at such normal VI sites vs. those characterized by preferential pathways. The conditions required for preferential pathways to be significant contributors to temporal variations in indoor air contaminant concentrations are also explored, and the consequences for sampling strategies are also discussed.

Methods

Statistical Analysis Of Field Data

To begin to characterize transient behavior in indoor air contaminant concentrations, actual datasets are analyzed to establish common levels of variability at VI sites. For this purpose, the datasets from the ASU house in Utah, the EPA Indianapolis site and North Island NAS were chosen for analysis. This paper relies on statistical analysis of published field data, and readers are referred to the original works for details regarding data acquisition.[3,5,8,9,17]

The ASU house and data were obtained over a period of a few years. During part of this time, controlled pressure method (CPM) tests were being conducted, in which the house was underpressurized to an extent greater than that characterizing "normal" operation. This caused greater than normal advective flow from the subsurface into the house, thus increasing VI potential.[6,8,18] This period of CPM testing is considered separately from the otherwise "natural" VI conditions in the analysis. Likewise, the existence of a preferential pathway at the ASU house needs to be considered in examining the dataset, noting that during some of the testing, this pathway was deliberately cut off, resulting in what we have termed "normal" VI conditions in which the main source of contaminant was believed to be groundwater.

The NAS North Island dataset has not (as far as is known) been influenced by a preferential pathway, but the structure there was subject to large internal pressure fluctuations, much more extensive than those typically recorded at the ASU house during normal operations. Additionally, the underlying soil at NAS North Island is sandy and more permeable than that at the ASU site, which, as will be shown, contributes to the indoor air contaminant concentrations being more sensitive to pressure fluctuations.[5]

Likewise, the Indianapolis site investigation spanned over a number of years and periodically included the testing of a sub-slab depressurziation system (SSD). The goal of which is to mitigate the VI risk by drastically depressurizing the sub-slab area underneath the house, preventing the contaminants from entering the structure above, and therefore only the period before the installation of this system was considered in the analysis. It is likely a sewer line beneath the structure acted as a preferential pathway,[11] however at no point was this PP removed, making it difficult to assess how significant the PP was at this site, regardless it is of interest to analyze this site due to its wealth of data.

The typical variation in indoor air contaminant concentrations with time will first be considered below in the case of the ASU house during "natural", (i.e. non-CPM conditions), in the case of the NAS North Island site over the entire available dataset, and for the Indianapolis case we consider the variations before the installation of the SSD system. The deviations from the mean TCE (Chloroform and PCE at the Indianapolis site) in indoor air concentration, as well as the indoor-outdoor pressure differential associated with these concentration fluctuations, were examined, and both univariate and bivariate kernel density estimations (KDE) were constructed. KDE is a technique that estimates the probability distribution of a random variable(s) by using multiple kernels, or weighting functions, and in this case, Gaussian kernels are used to create the KDEs. This means that it is presumed that the variables of interest (i.e., indoor air contaminant concentrations and indoor-outdoor pressure differentials, as sampled) are normally distributed around mean values (that there is statistical fluctuation associated with each sampling event). In this instance, the scipy statistical package was used to construct the KDEs, assuming a bandwidth parameter determined by Scott's rule. The distributions of the individual parameters and the relationship between them will be examined using the KDE method.

Modeling Work

In addition to examining the actual field data, a previously described three -dimensional computational fluid dynamics model of a generic VI impacted house was used to elucidate certain aspects of the processes. This model was implemented in a finite element solver, COMSOL Multiphysics. In the present work, there has been an addition of a preferential pathway to the "standard" model that has been described before in publications by this group.[19–21] In this modeling work, only the vadose zone soil domain is directly modeled.

The modeled structure is assumed to have a 10x10 m foundation footprint, with the bottom of the foundation slab lying 1 m below ground surface (bgs), simulating a house with a basement. The indoor air space is modeled as a continuously stirred tank (CST)[1] and all of the contaminant entering the house is assumed to enter with soil gas through a 1 cm wide crack located between the foundation walls and the foundation slab that spans the perimeter of the house. All of the contaminant leaving the indoor air space is assumed does so via air exchange with the ambient. The indoor control volume is assumed to consist of only of the basement, assumed as having a total volume of 300 m^3. Clearly different assumptions could be made regarding the structural features and the size of the crack entry route, but for present purposes, this is unimportant as the intent is only to show for "typical" values what the influence of certain other features can be. The modeled surrounding soil domain extends 5 meters from the perimeter of the house, and is assumed to consist of sandy clay (except as noted). Directly beneath the foundation slab, there is assumed to be a 30 cm (one foot) thick gravel layer, except in certain cases where this sub-base material is assumed to be the same as the surrounding soil (termed a "uniform" soil scenario). The preferential pathway is modeled as a 10 cm (4") pipe that exits into the gravel sub-base beneath the structure. The air in the pipe is assumed to be contaminated with TCE at a vapor concentration equal to the vapor in equilibrium with the groundwater contaminant concentration below the structure, modified by a scaling factor χ, which is allows the contaminant concentration in the pipe to be parameterized. The groundwater beneath the structure is assumed to be homogeneously contaminated with trichloroethylene (TCE) as a prototypical contaminant. The groundwater itself is not modeled, as the bottom of the model domain is defined by the top of the water table. The ground surface and the pipe are both assumed to be sources of air to the soil domain. Both are assumed to be at reference atmospheric pressure. Vapor transport in the soil is governed by Richard's equation, a modified version of Darcy's Law, taking the variability of soil moisture in the vadose zone into account.[22] The van Genuchten equations are used to predict the soil moisture content and thus the effective permeability of the soil.[23] The effective diffusivity of contaminant in soil is calculated using the Millington-Quirk model.[24] The transport of vapor contaminant in the soil is assumed to be governed by the advection-diffusion equation, in which either advection or diffusion may dominate depending upon position and particular circumstances. The equations and the boundary conditions are given in Table 1.

Drivers For Indoor Air Contaminant Variability

The Role Of Building Depressurization/Pressurization

Out of the factors that influence IACC in VI, pressure is one of the most dynamic ones, and the relationship between changes in indoor/outdoor pressure difference and IACC are examined in Figure 1. Three well-studied VI sites are considered, the "ASU house" near Hill AFB in Utah, a building at North Island NAS in California and a duplex in Indianapolis.

The absolute IACC at these sites vary significantly, therefore some means of comparing them all to each other is necessary. Additionally, the focus in this section is the driver for variations in IACC, and representation of the variations between the different sites must also be achieved, specifically variations on the scale of order of magnitudes is of the greatest interest, as these are the largest hinderance to proper site IACC characterization. To achieve these goals, the log-10 deviation from the mean IACC (μ) within each dataset is calculated, e.g. 10μ indicates the IACC is an order of magnitude above the mean IACC for the dataset. On the y-margin in figures 1a and 1b, the univariate KDE distribution of deviation from the mean may be seen.

The indoor/outdoor pressure differences are simply taken as it, and their univariate KDE distributions are shown on the x-margin. A negative pressure difference indicate that the building is underpressurized relative to outdoor.

The relationship between the deviation from mean IACC, and indoor/outdoor pressure difference may be seen in the central portion of each figure, in the form of a bivariate KDE

Table 1: Governing equations, boundary conditions & model input parameters. (See below for table of nomenclature).

(a) Governing equations

Unsteady-CSTR	$V\frac{du}{dt} = \int_{A_{\mathrm{ck}}} j_{\mathrm{ck}} dA - uA_eV$
Richard's equation	$\nabla \cdot \rho\Big(-\frac{\kappa_s}{\mu}k_r\nabla p\Big) = 0$
Millington-Quirk	$D_{\mathrm{eff}} = D_{\mathrm{air}}\frac{\theta_g^{10/3}}{\theta_t^2} + \frac{D_{\mathrm{water}}}{K_H}\frac{\theta_w^{10/3}}{\theta_t^2}$
Advection-diffusion equation	$\frac{\partial}{\partial t}\Big(\theta_w c_w + \theta_g c\Big) = \nabla(D_{\mathrm{eff}} \cdot \nabla c) - \vec{u} \cdot \nabla c$
van Genuchten equations	$\mathrm{Se} = \frac{\theta_w - \theta_r}{\theta_t - \theta_r} = [1 + \lvert\alpha z\rvert^n]^{-m}$ $\theta_g = \theta_t - \theta_w$ $k_r = (1-\mathrm{Se})^l[1-(\mathrm{Se}^{-m})^m]^2$ $m = 1 - 1/n$

(b) Boundary conditions

Boundary	**Richard's equation**	**Advection-diffusion equation**
At foundation crack	$p = p_{\mathrm{in/out}}$ (Pa)	$j_{\mathrm{ck}} = \frac{uc}{1-\exp(uL_{\mathrm{slab}}/D_{\mathrm{air}})}$
At groundwater source	N/A	$c = c_{\mathrm{gw}}K_H$ (μg/m^3)
At ground surface	$p = 0$ (Pa)	$c = 0$ (μg/m^3)
Exit of preferential pathway	$p = 0$ (Pa)	$c = c_{\mathrm{gw}}K_H\chi$ (μg/m^3)

(c) Soil & gravel properties[25–27]

Soil	Permeability (m^2)	Density (kg/m^3)	θ_s	θ_r	α (1/m)	n
Gravel	$1.3 \cdot 10^{-9}$	1680	0.42	0.005	100	3.1
Sand	$9.9 \cdot 10^{-12}$	1430	0.38	0.053	3.5	3.2
Sandy Clay	$1.7 \cdot 10^{-14}$	1470	0.39	0.12	3.3	1.2

(d) Trichloroethylene (diluted in air) properties[26,27]

D_{air} (m^2/h)	D_{water} (m^2/h)	Density (kg/m^3)	Viscosity (Pa $\cdot$ s)	K_H	M (g/mol)
$2.47 \cdot 10^{-2}$	$3.67 \cdot 10^{-6}$	1.614	$1.86 \cdot 10^{-5}$	0.403	131.39

(e) Building properties

V_{base} (m^3)	L_{slab} (cm)	A_e (1/hr)
300	15	0.5

distribution. The p-value and Pearson's r-value for each bivariate distribution is shown in the legend.

In Figure 1a the North Island and ASU house datasets are plotted, with blue representing

Figure 1: KDE analysis of IACC dependence on indoor/outdoor pressure difference at the ASU house and North Island site (1a) and the Indianapolis site (1b). p-values and Pearson's r-values shown for each dataset.

(a) Period before and after the PP was shut at the ASU house considered separately; North Island dataset considered in its entirety.

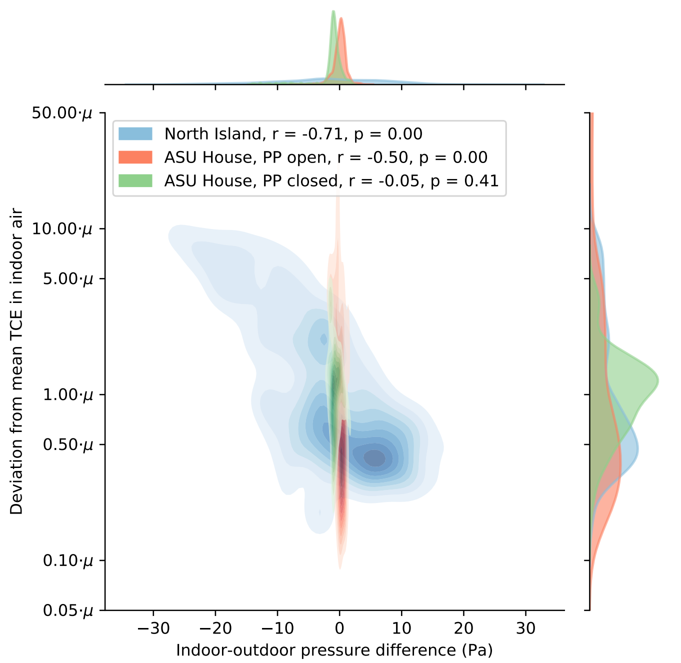

(b) Chloroform and PCE considered separeately at Indianapolis duplex 422.

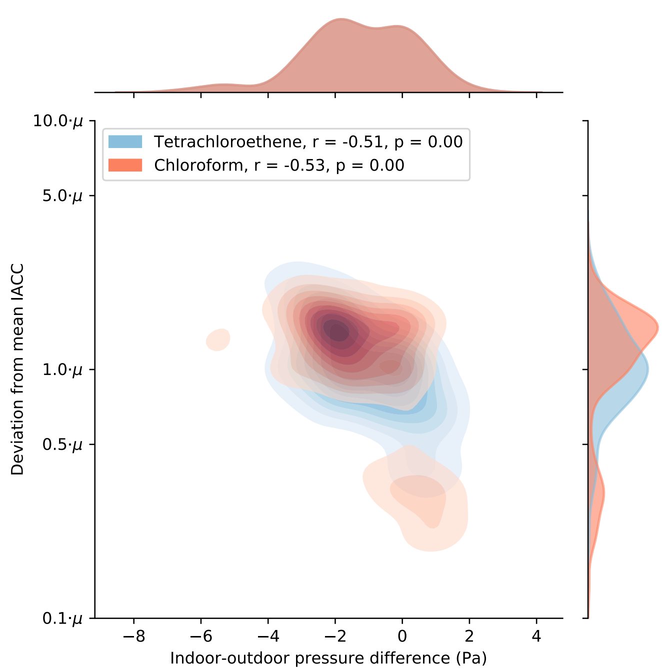

the North Island site, and with red and green representing the ASU house. The ASU house dataset is split into two different parts, the first (red) is data from the time period before the PP was discovered, the second (green) is from after the PP was sealed off. At both of these sites, TCE was the only contaminant considered. The IACC of Chloroform and PCE in the 422 part of the Indianapolis duplex are considered in Figure 1b.

From Figure 1a, it is apparent that the three datasets differ significantly from each other. The North Island site exhibit the greatest variation in both pressure difference and IACC, in fact, looking at the univariate pressure distribution - it is almost entirely flat and spanning from extremly high and low values. A likely explation for this is the poor condition of the structure, rendering it highly susceptible to envivornmental influnces.

To accompany this, there is significant variation in IACC, that has a relativly strong link with pressure difference ($r = -0.71$), although there is clearly a distinct peak (around 0.5μ) that is primally associated with the smaller negative and positive pressure differences ($-4 \leq \Delta p \leq 8$). This demonstrates that at this particular site, the very large variations (an order of magnitude or more) are primarily influenced by the unusually large pressure difference fluctations. Likely, this relationship is amplified by the fact that the soil surrounding the structure is sandy and therefore relatively permeable - increasing the influence of pressure differences. However, despite all this, pressure differences can only partly explain the variations observed at this site.

The two ASU datasets are not only significantly different from the North Island dataset, but also different from each other. Consider the dataset before the PP was discovered (red) and one can see that the IACC varies significantly (from 0.05μ to more than 50μ, albeit rarely.) This is more variation than was observed at North Island, and yet the distribution of pressure differences is narrow, mostly varying by a few Pa around zero (± 2 Pa), and with $r = -0.50$, suggests that pressure difference is not insignificant but still a weak predictor for the variations in IACC.

The picture changes completely after the PP was closed off, where a similar distribution of pressure differences is observed, but with a signficant reduction in IACC variance to around $\pm 0.5\mu$, resembling something of a log-normal distribution. This clearly shows just how much variance the PP at this site contributed with, and how critical it is to assess whether a PP is present at a particular site in general, lest potentially face unacceptable uncertainty in determining the relevant contaminant exposure. It is also clear that in the absence of a PP, the pressure difference becomes even less important, with the p- and r-value indicating that pressure differences are here insignficant in determining variation in IACC. This also suggests that the PP at the ASU house acted not only as a PP for contaminant vapors, but for air in general - allowing the impermeable soil surrounding the house to be circumvented. PPs, and the factors that influnce them will be explored later in this article.

The Indianapolis duplex also featured a PP, but despite this, there is significantly less variance in IACC of both Chloroform and PCE. The exact reason for this is not known, but considering that the PP at the Indianapolis site was a sanitary sewer, and at ASU the PP was a foundation drain system, it is not inconceivable that their dynamics are quite different. Nevertheless, both PCE and Chloroform are more or less log-normally distributed, with (mostly) less than an order of magnitude variance around the mean, indicating that the varation in IACC are species independent.

The pressure difference distribution exhibit some bimodal characteristics, with a larger variation than was observed at the ASU site. This may explain why the r-values for both PCE and Chloroform, $r = -0.51$ and $r = -0.53$ respectively, are so similar to the ASU site before the PP there was closed; the larger pressure differences, which occured more often than ASU, increase contaminant entry rates to the extent that a PP was needed to "achieve" at the ASU site.

All of these data clearly suggest that there is significant variation in IACC that cannot be easily explained by variations in indoor/outdoor pressure difference - even with a PP. It is also clear that PP may contribute with unacceptable levels of variations, and screening for PPs should be part of any site investiation. It may also be prudent, even in the absence of PP, to add around a half to one order of magnitude margin of error to early screening measurements of indoor air. E.g. if a single sample is less than an order of magnitude from some target limit, it may be justified to perform subsequent samples to better assess the relevant exposure. These data also call the role of advection in VI into question, as "normal" pressure difference ranges are such a poor predictor of IACC variation, which is the opposite of what one would expect if advection was a dominant transport mechanism.

The Role Of Air Exchange Rate

Air exchange rate, which measures how often the interior air in a given building is exchanged with exterior air, is the main parameter characterizing contaminant expulsion, and another highly dynamic process. Exploring the impact of fluctuations in air exchange rate is thus also important for the development of sampling strategies. At the ASU house, the contaminant entry rate into the structure (called emission rate in that study) as well as the building air exchange rate were recorded across time. This allows for exploration of the impact that fluctuating air exchange rate has on the final IACC by solving the CST equation, using the recorded contaminant entry rate as one input, and assuming a constant air exchange rate. The rationale is to show the extent of variability in IACC due to factors other than fluctuations in air exchange rates. We have taken this factor out of consideration by assuming a single constant exchange rate, characteristic of the whole period.

In Figure 2a, the measured IACC and air exchange rate across time are shown, with the predicted IACC assuming a constant air exchange rate. The median air exchange rate value for the pre-CPM period was chosen as this seemed to be the most representative value for this time period. From Figure 2a it may be seen quite clearly that for the non-CPM periods, the calculated IACC assuming constant and actual fluctuating exchange rates are quite similar. In other words, in this instance it is unlikely that the variations in IACC were driven by fluctuations in air exchange rate.

This is more clearly shown in Figure 2b, where KDEs of the IACC are constructed

Figure 2: Comparison between the recorded and the calculated TCE in indoor air at the ASU house, assuming constant air exchange rate. 2a shows the TCE in indoor air across time as well as the exchange rate. 2b shows the distribution of these values for three periods.

(a)

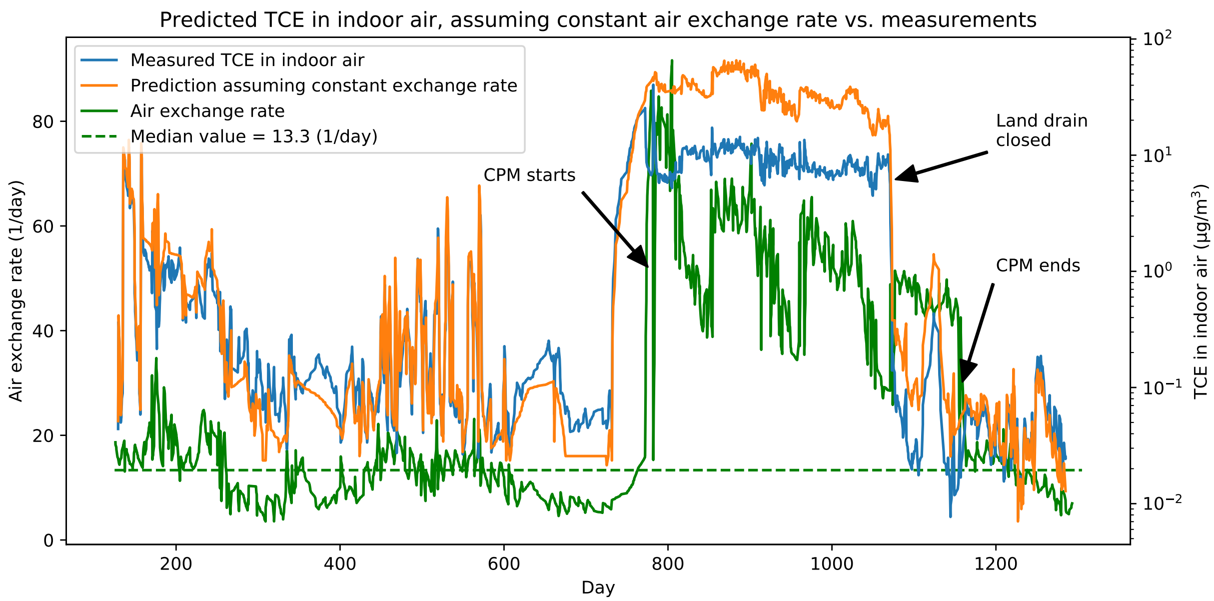

(b)

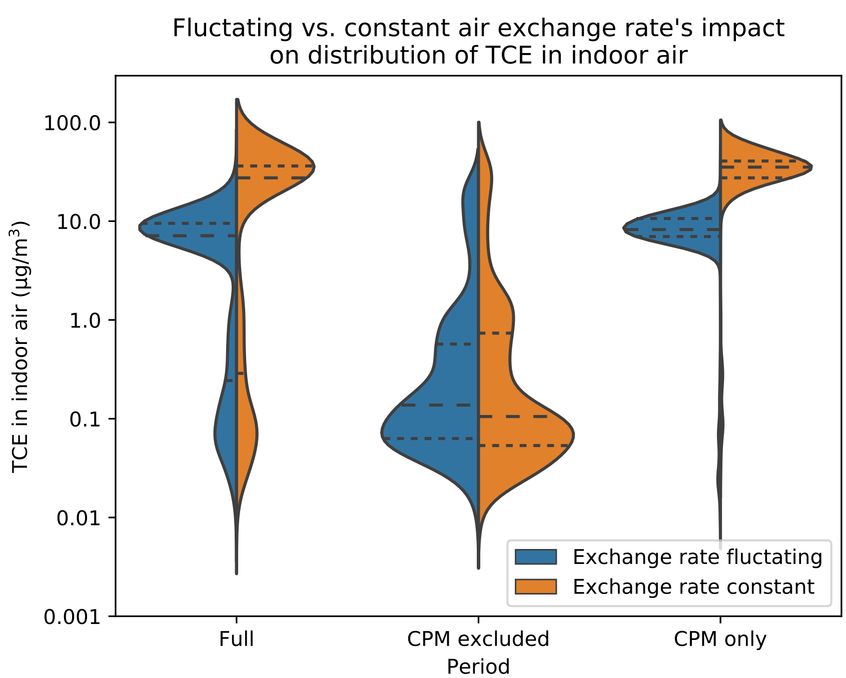

assuming the constant and fluctuating air exchange rate cases. This figure shows the relative probability of being at a particular TCE in indoor air concentration at the ASU house. These are compared to each other for 1. the full measurement period, 2. the non-CPM periods and 3. the CPM period. Looking at the full period, it does not appear as though the two cases of steady and fluctuating air exchange rate are comparable, the distribution functions for IACC are different and offset. The curves to the different sides of the vertical line for the "full" measurement period represent the probability distributions for the indicated values of IACC. It appears as though assuming a constant air exchange rate shifts the IACC probability distribution to higher values. The reason for this are more apparent when considering the CPM and non-CPM periods separately.

Considering only the CPM period, assuming a constant air exchange rate does not influence the shape of the IACC distribution, but assuming constant exchange rate shifts the IACC to a higher values. This is because the actual air exchange rate for this CPM period is significantly higher than the assumed median value, and much more contaminant is actually exchanged with the exterior. The shape of the IACC distribution is not very different from that which takes the air exchange fluctuations into account however, indicating that fluctuating exchange rate is not a major contributor to observed IACC variation for this period (the distinction being drawn between variation and absolute levels of IACC).

The non-CPM period is the condition under which field practitioners would normally collect samples at a VI site. It is clear here that there is only a very minor difference made in assuming a constant vs. real fluctating air exchange rate, again indicating that account for the minor fluctuations of air exchange rate's impact on variations in IACC is not important. Rackes and Waring[28] drew similar conclusions regarding the relationship between IACC and air exchange rate.

The Influence of Preferential Pathways

Conclusions From Steady-State Modeling

Clearly, PPs pose a major problem for site investigations, in particular because they may be difficult or even impossible to anticipate or uncover; even at a well studied site like the

Figure 3: Sensitivity analysis of IACC dependence on indoor/outdoor pressure difference for cases featuring a PP (3a) and without a PP (3b). Results compared with field data from ASU house.

(a) PP present. Sensitivity to the presence of a gravel sub-base and contamination in the PP considered.

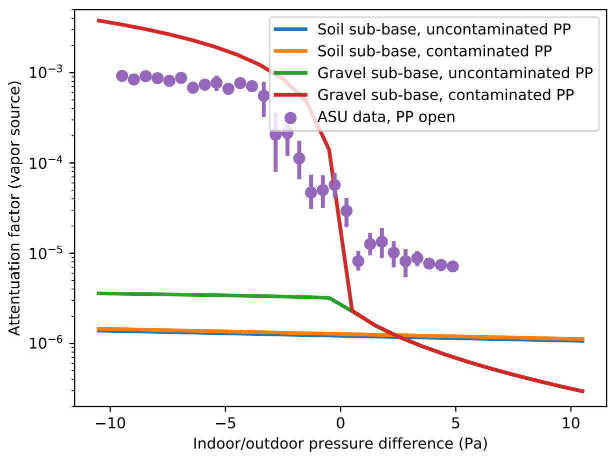

(b) No PP present. Sensitivitiy to the presence of a gravel sub-base considered.

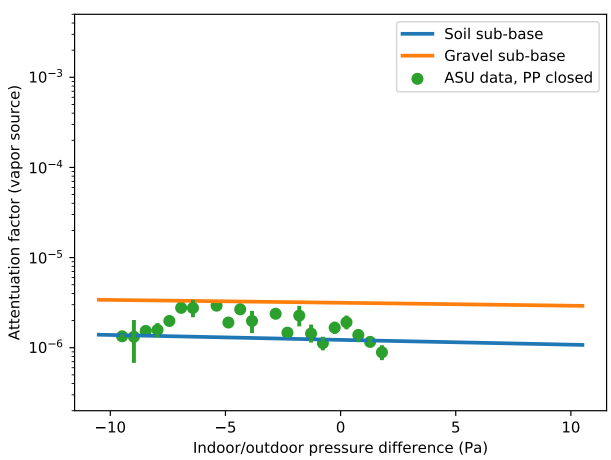

ASU house it took years to discover the PP. Therefore, there is a need to consider other indications that a PP is present or a potential issue.

To investigate this, inspiration is taken from the ASU house, where there clearly was a PP containing contaminant vapor, which exited into a gravel (permeable) sub-base. The impact of these features is simulated by examining the IACC at different indoor/outdoor pressure differences for each combination of cases. Instead of representing IACC as absolute concentration, we now non-dimensionalize with respect to the vapor in equilibrium with the groundwater contaminant concentration. This non-dimensionalized property is commonly called the attenuation factor and is denoted by α_{gw}. The result of a steady-state sensitivity analysis relative to several factors is seen in Figure 3.

Figure 3a deal with cases where a PP is present and, the impact of having a gravel vs. soil sub-base and vapor contaminant vs. clean air in the PP ($\chi = 1$ and $\chi = 0$ respectively) are considered. Figure 3b considers the cases absent a PP, for reference, but still considers the impact of a gravel vs. soil sub-base. To validate these results, the IACC at the ASU house (as α_{gw}) vs. indoor/outdoor pressure difference are also plotted. Only data from period before the PP was discovered, and after the PP was closed are considered in each respective figure (3a and 3b). To improve visibility of the ASU data, it's average α_{gw} are aggregated into up to 40 evenly spaced bins on the x-axis.

Begining with Figure 3a it immediately clear that absent a gravel sub-base, the impact of a PP is minimal, as the orange and blue lines show. Since in the model, it is assumed that the soil type is sandy clay, which is relatively impermeable, there is simply too much resistance to advection for changes in pressurization to matter. Additionally, whether the PP is filled with contaminant vapors or not does matter; without a permeable sub-base, the transport of contaminant vapor in the sub-base is too inhibited to be effectively transported into the building.

Moving on to the case of when a gravel sub-base is present, and the PP is filled with contaminant vapors ($\chi = 1$). In this scenario the PP has a massive impact on α_{gw}, spanning more than four orders of magnitude. This is explained by the increased role of advective transport under these conditions. The gravel sub-base allows vapor to flow more easily, and the PP is able to circumvent the large resistance to transport due to the surrounding soil, realizing the advective potential offered by the gravel sub-base. When the building is underpressurized under these conditions, a significant amount of contaminant vapor is able to be pulled from the PP, leading to the large increase of α_{gw}.

On the other hand, due to the increased advective potential, overpressurization more effectively prevents contaminant vapors from entering the structure, and most of the contaminant entering the building does so through diffusion. This also explains why there is no difference between the uncontaminted and contaminted PP cases (red and green) when the building is overpressurized. But these two cases (red and green) differ signficant when the building is underpressurized, obviously because there simply is no additional contaminant being supplied by the PP, α_{gw} thus limits to whatever diffuses from the contaminted groundwater source.

It is interesting to note that α_{gw} is higher with an uncontaminted PP (green) than the cases without a gravel sub-base. One could expect that pulling so much clean air into the sub-base region would significantly dilute the contaminant vapors and if anything cause a decrease in α_{gw} relative to blue and orange. However, the PP is small relative to the sub-base (10 cm diameter pipe), thus impacting the contaminant concentration in a limited region of the sub-base, but still allows for higher advection in the entire sub-base region, leading to a α_{gw} plateau that is limited by contaminant transport from the groundwater source.

These case most resembling the ASU site (with an open PP) is the red case, and fits the data fairly well, especially for small under-/overpressurization values. The most significant deviations occur as the under-/overpressurization becomes larger. However, the model is not intended to replicate the ASU data perfectly, but rather investigate the factors make a PP the most impactful in a general sense, and perfect simulation is not to be expected. This is especially reflected in the choice of vapor contaminant concentration in the PP, with it either being equal to the groundwater contaminant vapor concentration ($\chi = 1$) or clean ($\chi = 0$), neither of which is likely to be true at the ASU site. The idea with picking $\chi = 1$ and $\chi = 0$ is to give a span of α_{gw} values that one can may expect a PP to fall between. Thus, this helps explain why α_{gw} is overpredicted when the structure is increasingly underpressurized - the contaminant vapor in the PP at the ASU house was lower than the groundwater contaminant vapor concentration. This does not explain why underprediction occurs at increasing overpressurization, but it is likely due to the steady-state nature of the simulations. Regardless, the simulation are able to capture the general trends well, with not too significant deviation, giving validity to the cases simulated.

In Figure 3b cases where a PP is absent are considered, i.e. a "normal" VI scenario, which may be considered reference scenarios. Here the only cases considered is whether there is a gravel or soil sub-base. It is apparent that without a PP, the indoor/outdoor pressure difference changes do not cause any signficant change in α_{gw}, due to the resistance to advective transport in the surrounding soil - showing the importance of the PP for increasing advection. Furthermore, the gravel sub-base does increase the overall α_{gw}, partly due to slightly higher advective potential but also due to the contaminant vapors more easily diffuse in the more permeable sub-base. The data from the ASU house after the PP there had been close agrees well with these model predictions, clearly again demonstrating the role of PP in increasing advective potential at a site. It should also be stated that if the surrounding soil was more permeable, e.g. sand, there would be more of a relationship between α_{gw} and pressurization.

Based on the simulated cases in Figure 3 it can be concluded that a PP can be a signficant contributor to VI, but only when some conditions are met.

1. The PP has to supply additional vapor contaminant.
2. There must be a source of increased advective potential, which may be due to the PP itself, or other site features or simply due to more permeable surrounding soil.
3. A permeable sub-base must exist to realize this advective potential.

In the absense of one or all of these conditions, a PP is unlikely to be a signficant contributor to VI. In lieu of actually uncovering an actual PP at a site, it may be easier for a site investigator to look for the above criteria. Strategies for screening for PP is also discussed by Nielsen and Hvidberg.[15]

Acknowledgement

This project was supported by grant ES-201502 from the Strategic Environmental Research and Development Program and Environmental Security Technology Certification Program (SERDP-ESTCP).

Table 2: Abbreviations & symbols

Abbreviation or symbol	**Explanation**
VI	Vapor intrusion
PP	Preferential pathway
L_{slab}	Thickness of the foundation concrete slab
p	Pressure
u	TCE in indoor air concentration
c	TCE in soil gas concentration
D_{air}	Diffusion of TCE in air
D_{water}	Diffusion of TCE in water
D_{eff}	Effective Diffusion of TCE in soil
K_H	Henry's Law constant
θ_g, θ_w & θ_s	Vapor, water filled & saturated soil porosity
θ_r	Residual moisture porosity
α, l, n & m	van Genuchten parameters
Se	Soil moisture saturation
k_r	Relative permeability
α_{gw}	Attenuation factor

References

(1) U.S. Environmental Protection Agency, OSWER Technical Guide for Assessing and Mitigating the Vapor Intrusion Pathway From Subsurface Vapor Sources To Indoor Air. `https://www.epa.gov/sites/production/files/2015-09/documents/oswer-vapor-intrusion-technical-guide-final.pdf`, 00005.

(2) Folkes, D.; Wertz, W.; Kurtz, J.; Kuehster, T. Observed Spatial and Temporal Distributions of CVOCs at Colorado and New York Vapor Intrusion Sites. *29*, 70–80, 00048.

(3) Holton, C.; Luo, H.; Dahlen, P.; Gorder, K.; Dettenmaier, E.; Johnson, P. C. Temporal

Variability of Indoor Air Concentrations under Natural Conditions in a House Overlying a Dilute Chlorinated Solvent Groundwater Plume. *47*, 13347–13354, 00028.

(4) Johnston, J. E.; Gibson, J. M. Spatiotemporal Variability of Tetrachloroethylene in Residential Indoor Air Due to Vapor Intrusion: A Longitudinal, Community-Based Study. *24*, 564, 00018.

(5) Hosangadi, V.; Shaver, B.; Hartman, B.; Pound, M.; Kram, M. L.; Frescura, C. High-Frequency Continuous Monitoring to Track Vapor Intrusion Resulting From Naturally Occurring Pressure Dynamics. *27*, 9–25, 00001.

(6) McHugh, T.; Loll, P.; Eklund, B. Recent Advances in Vapor Intrusion Site Investigations. *204*, 783–792, 00005.

(7) Johnson, P. C.; Holton, C. W.; Guo, Y.; Dahlen, P.; Luo, E. H.; Gorder, K.; Dettenmaier, E.; Hinchee, R. E. Integrated Field-Scale, Lab-Scale, and Modeling Studies for Improving Our Ability to Assess the Groundwater to Indoor Air Pathway at Chlorinated Solvent-Impacted Groundwater Sites. 00003.

(8) Holton, C. W. Evaluation of Vapor Intrusion Pathway Assessment Through Long-Term Monitoring Studies. `https://repository.asu.edu/attachments/150778/content/Holton_asu_0010E_15040.pdf`, 00003.

(9) Guo, Y. Vapor Intrusion at a Site with an Alternative Pathway and a Fluctuating Groundwater Table. `https://repository.asu.edu/items/36435`, 00001.

(10) Guo, Y.; Holton, C.; Luo, H.; Dahlen, P.; Gorder, K.; Dettenmaier, E.; Johnson, P. C. Identification of Alternative Vapor Intrusion Pathways Using Controlled Pressure Testing, Soil Gas Monitoring, and Screening Model Calculations. *49*, 13472–13482, 00019.

(11) McHugh, T.; Beckley, L.; Sullivan, T.; Lutes, C.; Truesdale, R.; Uppencamp, R.;

Cosky, B.; Zimmerman, J.; Schumacher, B. Evidence of a Sewer Vapor Transport Pathway at the USEPA Vapor Intrusion Research Duplex. *598*, 772–779, 00007.

(12) Pennell, K. G.; Scammell, M. K.; McClean, M. D.; Ames, J.; Weldon, B.; Friguglietti, L.; Suuberg, E. M.; Shen, R.; Indeglia, P. A.; Heiger-Bernays, W. J. Sewer Gas: An Indoor Air Source of PCE to Consider During Vapor Intrusion Investigations. *33*, 119–126, 00022.

(13) Roghani, M.; Jacobs, O. P.; Miller, A.; Willett, E. J.; Jacobs, J. A.; Viteri, C. R.; Shirazi, E.; Pennell, K. G. Occurrence of Chlorinated Volatile Organic Compounds (VOCs) in a Sanitary Sewer System: Implications for Assessing Vapor Intrusion Alternative Pathways. *616-617*, 1149–1162, 00001.

(14) Riis, C. E.; Christensen, A. G.; Hansen, M. H.; Husum, H.; Terkelsen, M. Vapor Intrusion through Sewer Systems: Migration Pathways of Chlorinated Solvents from Groundwater to Indoor Air. Seventh International Conference on Remediation of Chlorinated and Recalcitrant Compounds. 00012.

(15) Nielsen, K. B.; Hvidberg, B. Remediation Techniques for Mitigating Vapor Intrusion from Sewer Systems to Indoor Air. *27*, 67–73, 00002.

(16) Brenner, D. Results of a Long-Term Study of Vapor Intrusion at Four Large Buildings at the NASA Ames Research Center. *60*, 747–758, 00003.

(17) U.S. Environmental Protection Agency, Assessment of Mitigation Systems on Vapor Intrusion: Temporal Trends, Attenuation Factors, and Contaminant Migration Routes under Mitigated And Non-Mitigated Conditions. 00002.

(18) McHugh, T. E.; Beckley, L.; Bailey, D.; Gorder, K.; Dettenmaier, E.; Rivera-Duarte, I.; Brock, S.; MacGregor, I. C. Evaluation of Vapor Intrusion Using Controlled Building Pressure. *46*, 4792–4799, 00037.

(19) Shen, R.; Pennell, K. G.; Suuberg, E. M. Influence of Soil Moisture on Soil Gas Vapor Concentration for Vapor Intrusion. *30*, 628–637, 00015 WOS:000325689400005.

(20) Yao, Y.; Wang, Y.; Zhong, Z.; Tang, M.; Suuberg, E. M. Investigating the Role of Soil Texture in Vapor Intrusion from Groundwater Sources. *46*, 776–784, 00003.

(21) Yao, Y.; Mao, F.; Ma, S.; Yao, Y.; Suuberg, E. M.; Tang, X. Three-Dimensional Simulation of Land Drains as a Preferential Pathway for Vapor Intrusion into Buildings. *46*, 1424–1433, 00002.

(22) Richards, L. A. Capillary Conduction of Liquids through Porous Mediums. *1*, 318–333, 05183.

(23) van Genuchten, M. T. A Closed-Form Equation for Predicting the Hydraulic Conductivity of Unsaturated Soils. *44*, 892–898, 00004.

(24) Millington, R. J.; Quirk, J. P. Permeability of Porous Solids. *57*, 1200, 01813.

(25) Dan, H.-C.; Xin, P.; Li, L.; Li, L.; Lockington, D. Capillary Effect on Flow in the Drainage Layer of Highway Pavement. *39*, 654–666, 00007.

(26) Abreu, L. D. V.; Schuver, H. Conceptual Model Scenarios for the Vapor Intrusion Pathway. `https://www.epa.gov/sites/production/files/2015-09/documents/vi-cms-v11final-2-24-2012.pdf`, 00010.

(27) U.S. Environmental Protection Agency, Users's Guide For Evaluating Subsurface Vapor Intrusion Into Buildings. `https://www.epa.gov/sites/production/files/2015-09/documents/2004_0222_3phase_users_guide.pdf`, 00000.

(28) Rackes, A.; Waring, M. S. Do Time-Averaged, Whole-Building, Effective Volatile Organic Compound (VOC) Emissions Depend on the Air Exchange Rate? A Statistical Analysis of Trends for 46 VOCs in U.S. Offices. *26*, 642–659, 00000.